An ab Initio Study of the Transition State and Forward and Reverse Rate Constants for $C_2H_5 \rightleftharpoons H + C_2H_4$

William L. Hase* and H. Bernhard Schlegel

Department of Chemistry, Wayne State University, Detroit, Michigan 48202

Vsevolod Balbyshev and Michael Page

Department of Chemistry, North Dakota State University, Fargo, North Dakota 58105

Received: September 28, 1995; In Final Form: January 15, 1996[⊗]

Different levels of ab initio theory are used to calculate geometries, vibrational frequencies, and energies for stationary points on the $H + C_2H_4 \rightleftharpoons C_2H_5$ potential energy surface. Frequencies and geometries calculated for C_2H_4 at the QCISD/6-311G** and MRCI/cc-pVDZ levels of theory are in very good agreement with experiment. The ab initio normal modes for the H- - -C_2H_4 transition state are similar to those for C_2H_4, and ratios between the C_2H_4 experimental anharmonic frequencies and ab initio harmonic frequencies are used to estimate anharmonic frequencies for the transition state. Nine of the 10 frequencies assigned for C_2H_5 from experiment are consistent with the ab initio calculations. The CC stretch was apparently misassigned and reassigned here. The ab initio calculations do not give definitive values for the $H + C_2H_4 \rightarrow C_2H_5$ barrier height and heat of reaction. Using these two energy terms as adjustable parameters in concert with the above stationary point geometries and frequencies, transition state theory (TST) rate constants are calculated for $H + C_2H_4 \rightarrow C_2H_5$ recombination and $C_2H_5 \rightarrow H + C_2H_4$ dissociation in the high-pressure limit. A $H + C_2H_4 \rightarrow C_2H_5$ barrier height of 3.0−3.1 kcal/mol gives TST recombination rate constants in excellent agreement with experiment. Because of the uncertainty in the experimental $C_2H_5 \rightarrow H + C_2H_4$ rate constant, a definitive value could not be deduced for the dissociation barrier from the TST fits to the experimental dissociation rate constants. Some of the experimentally determined dissociation *A* factors are more than an order of magnitude smaller than the TST value.

I. Introduction

There have been extensive experimental[1−12] and theoretical[13−22] studies of the kinetics of the $C_2H_5 \rightleftharpoons H + C_2H_4$ reactive system. One of the goals of this work is to determine whether the reaction can be adequately interpreted by the RRKM and transition state theories. It is important to know whether these theories are adequate for reactions as elementary and important as C_2H_5 dissociation and $H + C_2H_4$ recombination (i.e., Figure 1).

The experimental data for the $C_2H_5 \rightleftharpoons H + C_2H_4$ system include the rate constant for C_2H_5 dissociation versus temperature and pressure,[6−12] and high-pressure $H + C_2H_4$ recombination rate constant versus temperature,[2−5] and the pressure dependence of this recombination rate constant.[1] There has been an extensive discussion in the literature concerning the ability of RRKM and transition state theory to simultaneously fit these rates in a consistent fashion.[23] Using the results of ab initio calculations, Hase and Schlegel (HS) proposed a transition state model for $C_2H_5 \rightleftharpoons H + C_2H_4$,[20] which appeared to give an acceptable fit to all the available experimental data. This model required the "high" value of 28.0 ± 1.0 kcal/mol for the 300 K C_2H_5 heat of formation,[24] to give a 0 K heat of reaction of 35.5 ± 1.0 kcal/mol. The C_2H_5 dissociation and $H + C_2H_4$ association thresholds were 38.0 and 2.5 kcal/mol, respectively, and quantum mechanical tunneling was included via the Wigner correction. The use of the above "high" value for $\Delta H_{f,298}(C_2H_5)$ has been supported by more recent experiments, and a weighted average of all the higher values of $\Delta H_{f,298}(C_2H_5)$ gives 28.4 ± 0.1 kcal/mol.[5]

Two recent articles[5,12] have reassessed the kinetics of the $C_2H_5 \rightleftharpoons H + C_2H_4$ system. In one,[5] similar reaction parameters were deduced as by HS; i.e., the same transition state structure was used, and values of 34.8 and 2.2 kcal/mol were adopted for the heat of reaction and $H + C_2H_4$ threshold, respectively. A different conclusion was reached in the second study.[12] Though the same C_2H_5 dissociation threshold of 38.0 kcal/mol was used as in the first study, it was concluded that a "tighter" transition state is required than that used by HS. In particular, the two H- - -C═C bending frequencies about the rupturing bond were proposed to be 500 and 700 cm^{-1}, instead of the values of 369 and 399 cm^{-1} proposed by HS.

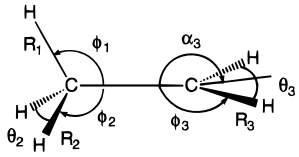

Figure 1. Coordinates used to define the geometry of C_2H_5 and the transition state.

Because of the questions concerning the proper transition state and energies for the $C_2H_5 \rightleftharpoons H + C_2H_4$ system, more definitive analyses of the reaction kinetics are in order. In this paper high-level ab initio calculations are reported of the transition state structure and reaction energetics. This information is then used in transition state theory calculations of the high-pressure C_2H_5 decomposition and $H + C_2H_4$ recombination rate constants versus temperature. Since the proper treatment of rotational angular momentum is critical for calculating either of these rate constants at intermediate and low pressures[25,26] and the correct treatment is currently unknown, the rate constant analyses presented here are restricted to the high-pressure limit.

[⊗] Abstract published in *Advance ACS Abstracts,* March 1, 1996.

0022-3654/96/20100-5354$12.00/0

TABLE 1: Ab Initio Minimum-Energy Geometries[a]

	6-31G*			6-311G**		6-311+G(2df,p)		
coord[b]	HF	MP2	QCISD	MP2	QCISD	MP2	CASSCF/DZP	MRCI/cc-pVDZ
					C_2H_4[c]			
R_{CC}	1.317	1.335	1.338	1.336	1.339	1.329	1.3645	1.346
R_{CH}	1.076	1.085	1.088	1.085	1.087	1.083	1.077	1.093
ϕ_{HCC}	121.8	121.7	121.8	121.4	121.6	121.5	121.5	121.6
					TS			
R_{CC}	1.358	1.339	1.358	1.333	1.353	1.327	1.370	1.362
R_1	2.003	1.834	1.903	1.867	1.976	1.842	1.885	1.939
R_2	1.075	1.084	1.088	1.084	1.087	1.082	1.076	1.092
R_3	1.075	1.084	1.088	1.084	1.087	1.081	1.076	1.092
ϕ_1	106.3	107.5	107.4	107.2	106.7	107.1	108.7	107.2
ϕ_2	121.2	121.1	121.1	121.1	121.1	121.2	120.5	121.1
ϕ_3	121.5	121.6	121.6	121.4	121.4	121.5	121.2	121.4
θ_2	116.5	116.0	116.2	116.6	116.8	116.5	116.5	116.6
θ_3	117.0	116.6	116.7	117.1	117.1	116.9	117.3	117.1
α_3	177.4	176.9	176.7	177.3	177.2	177.6	174.8	176.8
					C_2H_5			
R_{CC}	1.498	1.498	1.495	1.492	1.499	1.482	–[d]	–
R_1	1.091	1.100	1.104	1.099	1.103	1.097	–	–
R_2	1.086	1.093	1.097	1.093	1.096	1.091	–	–
R_3	1.075	1.082	1.087	1.082	1.086	1.079	–	–
ϕ_1	111.7	111.9	111.9	111.6	111.6	111.7	–	–
ϕ_2	111.3	111.4	111.4	111.4	111.3	111.7	–	–
ϕ_3	120.4	120.7	120.8	120.5	120.5	120.9	–	–
θ_2	108.0	108.1	108.1	108.2	108.3	108.1	–	–
θ_3	117.3	117.2	117.3	117.5	117.6	117.5	–	–
α_3	166.4	168.3	169.7	168.1	169.0	171.5	–	–

[a] Distances are in angstroms and angles are in degrees. [b] The coordinates are defined in Figure 1. [c] The experimental geometry for C_2H_4 is R_{CC} = 1.339 Å, R_{CH} = 1.085 Å, and ϕ_{HCC} = 121.1°.[37] [d] (–) means the geometry was not calculated.

II. Ab Initio Calculations

Two separate approaches were employed to calculate features of the potential energy surface for the $C_2H_5 \rightleftharpoons H + C_2H_4$ reactive system, to strengthen the validity of the conclusions of the study. In the first approach single reference determinant calculations were used with large basis sets and high levels of theory. The 6-31G(d), 6-311G(d,p), and 6-311+G(2df,p) basis sets were used.[27] Energies were calculated by spin unrestricted second-order Møller−Plesset perturbation theory (MP2),[28] spin projected fourth-order Møller−Plesset perturbation theory (PMP4),[29] quadratic configuration interaction (QCISD), and quadratic configuration interaction with perturbative correction for triplet excitations (QCISD(T)).[30] Geometries were optimized at the MP2 and QCISD levels of theory. Vibrational frequencies were computed from analytic second derivatives at the MP2 level and from numerical second derivatives at the QCISD level. These calculations were carried out with the Gaussian 92 series of programs.[31]

In the second approach spin restricted complete active space multiconfiguration SCF (CASSCF) and multireference configuration interaction (MRCI) calculations were employed. The simplest qualitatively correct complete active space (CASSCF)[32] reference description for the title reaction includes three electrons distributed among three molecular orbitals. At $H + C_2H_4$, these three orbitals include the C−C π-bonding and antibonding orbitals as well as the radical orbital on the hydrogen atom. At C_2H_5, they include the methylene carbon atom radical orbital as well as the σ-bonding and antibonding orbitals for the C−H bond adjacent to the radical. The resulting 3-in-3 CASSCF reference wave function includes eight doublet configurations. Calculations were also performed with a larger active space that includes the C−C σ-bonding and antibonding orbitals. The resulting 5-in-5 CASSCF reference wave function includes 75 doublet configurations.

The molecular orbitals generated at the reference CASSCF level are used in large-scale multireference configuration (MRCI) calculations to include the effects of dynamical electron correlation. For all of the MRCI calculations reported here, the 1s core orbitals on both carbon atoms are restricted to be doubly occupied, and no excitations are included into the two highest energy virtual orbitals. Other than this restriction, the MRCI calculations include all spin-adapted configurations generated as single- or double-electron replacements from any of the CASSCF reference configurations.

Four basis sets are used for the CASSCF and MRCI calculations, denoted DZP, cc-pVDZ, TZ2P, and TZ2P+F. The DZP basis set is the standard Dunning 4s/2p contraction[33] of the 9s/5p primitive set of Huzinaga[34] on carbon and the corresponding unscaled 4s to 2s contraction on hydrogen, augmented with a set of d functions on carbon and a set of p functions on hydrogen both with exponents of 0.75. The three other basis sets are based on Dunning's correlation consistent basis sets.[35] The cc-pVDZ basis set consists of a (9s5p1d) primitive set contracted to [3s2p1d] for carbon and a (4s) primitive set contracted to [2s] augmented with a (1p) for hydrogen. The TZ2P basis set is obtained by removing the f function and the d function from hydrogen from the correlation consistent polarized valence triple-zeta (cc-pVTZ) basis sets of Dunning.[35] These are composed of a (10s5p2d1f) primitive set contracted to [4s3p2d1f] for carbon and a (5s) set contracted to [3s] and augmented by a (2p1d) polarization set for hydrogen. The TZ2P+F basis set consists of the cc-pVTZ excluding only the d functions on hydrogen. All CASSCF and MRCI calculations have been carried out using the MESA[36] system of programs.

A. Geometries. As shown in Table 1, there is very good agreement between all the levels of theory for the changes in geometry on going from reactants to the transition state to products. The calculated geometry of ethylene is in very good agreement with the experimental structure (R_{CC} = 1.339 Å, R_{CH} = 1.085 Å, ϕ_{HCC} = 121.1 Å).[37] For ethyl radical we see the same shortening of the CC and α CH bonds and lengthening of

TABLE 2: Ab Initio Vibrational Frequencies[a]

6-31G*			6-311G**		6-311+G(2df,p)			
HF	MP2	QCISD	MP2	QCISD	MP2	QCISD[b]	CASSCF/DZP	MRCI/cc-pVDZ
				C_2H_4[a]				
897.0	850.8	846.2	827.6	830.2	831.9	834.5[b]	856.0	837.6
1095.0	942.1	935.3	915.5	921.6	969.1	975.2	879.3	910.9
1099.4	990.3	977.2	970.8	967.5	985.5	982.2	931.5	957.6
1154.9	1085.3	1057.1	1073.5	1053.7	1073.0	1053.2	1077.0	1049.4
1352.5	1265.8	1258.9	1235.7	1240.9	1248.2	1253.3	1329.0	1257.9
1496.9	1415.4	1401.7	1384.9	1381.3	1385.4	1381.8	1422.1	1378.0
1610.2	1521.0	1509.8	1480.5	1485.6	1482.9	1488.1	1581.3	1482.3
1856.2	1720.7	1716.7	1683.1	1690.7	1685.0	1692.6	1749.8	1692.8
3320.9	3213.7	3168.6	3183.3	3152.3	3180.6	3149.6	3304.8	3214.2
3344.2	3231.0	3187.8	3201.0	3171.5	3196.9	3167.4	3323.9	3222.7
3394.6	3300.4	3245.6	3273.3	3233.8	3269.6	3230.0	3392.5	3301.2
3420.6	3323.0	3268.7	3299.5	3259.7	3295.9	3256.1	3418.5	3320.8
				TS				
657.9i	1212.7i	968.1i	1157.5i	822.5i	1195.0i	860.0i	1187.7i	900.2i
414.0	501.0	445.2	443.6	373.9	460.7	391.0	469.3	404.3
445.4	527.1	473.7	472.0	405.9	498.0	431.9	501.1	427.7
881.1	857.2	840.7	838.5	827.6	839.3	828.6	838.0	831.6
929.5	987.4	901.2	996.7	907.6	1026.3	937.1	868.2	882.3
1026.0	1106.0	1022.9	1067.8	982.8	1106.8	1021.9	1024.2	973.1
1037.8	1125.4	1045.7	1118.6	1036.6	1132.0	1050.0	1054.9	1030.6
1320.7	1282.1	1260.6	1253.9	1242.3	1261.9	1250.4	1327.0	1255.7
1340.0	1384.6	1352.8	1374.2	1345.6	1379.2	1350.6	1344.5	1342.5
1600.2	1527.8	1506.2	1490.4	1483.9	1491.2	1484.7	1576.7	1480.6
1693.0	1677.4	1643.8	1664.4	1632.1	1672.0	1639.8	1686.1	1633.1
3326.9	3228.8	3177.6	3197.7	3159.0	3195.5	3156.8	3311.7	3223.8
3339.4	3240.1	3190.2	3209.7	3172.8	3206.8	3169.9	3323.4	3225.4
3406.6	3316.3	3257.3	3288.4	3243.1	3284.4	3239.0	3401.5	3308.4
3431.5	3340.0	3279.7	3314.6	3267.7	3311.2	3264.3	3426.2	3327.1
				C_2H_5				
168.7	156.8	146.0	161.3	149.8	133.1	121.7[b]	–	–
460.3	461.4	456.8	463.4	454.9	481.6	473.0	–	–
871.2	837.8	831.3	821.1	815.5	821.4	815.7	–	–
1083.4	1027.7	1023.1	1000.0	1001.7	993.4	995.2	–	–
1112.9	1086.3	1093.1	1094.3	1076.8	1093.5	1076.0	–	–
1309.3	1244.9	1233.4	1218.4	1214.2	1212.0	1207.8	–	–
1552.6	1467.8	1457.5	1422.0	1425.1	1418.9	1421.9	–	–
1608.8	1535.9	1517.2	1496.1	1492.0	1495.7	1491.6	–	–
1629.9	1551.1	1533.8	1509.9	1506.1	1509.1	1505.2	–	–
1635.1	1558.6	1540.3	1511.2	1508.5	1510.3	1507.6	–	–
3159.5	3068.7	3014.0	3044.2	3033.4	3037.3	2996.5	–	–
3228.5	3154.2	3093.9	3128.6	3082.2	3121.9	3075.5	–	–
3263.4	3199.1	3135.9	3174.0	3124.6	3169.0	3119.6	–	–
3313.5	3244.4	3184.8	3213.5	3165.2	3217.2	3168.9	–	–
3411.5	3353.1	3283.6	3324.5	3268.3	3328.2	3272.1	–	–

[a] The frequencies are in units of cm^{-1}. The experimental[39] harmonic frequencies for C_2H_4 are listed in section II.B. [b] These QCISD frequencies are estimated by using the frequencies from QCISD/6-311G** + [MP2/6-311+G(2df,p) − MP2/6-311G**]. [c] (−) means the frequencies was not calculated.

the anti β CH bond as noted by Pacansky and Dupuis.[38] In the transition state, the C_2H_4 moiety resembles ethylene. At the QCI and MRCI levels R_{CC} is only *ca.* 0.015 Å longer than in ethylene, and the tricoordinate carbon is still nearly planar. The distance for the attacking/departing hydrogen, R_1, is ca. 1.95 Å at the highest levels of theory (QCI and MRCI); the MP2 and CASSCF methods seem to underestimate this distance by about 0.1 Å. The bond angles are quite consistent across all levels of theory considered.

B. Vibrational Frequencies. The calculated vibrational frequencies for C_2H_4, the transition state, and C_2H_5 are listed in Table 2. Experimental harmonic frequencies have been reported for C_2H_4, by applying Dennison's correction to the measured anharmonic frequencies.[39] These harmonic frequencies, in ascending order, are 842.9, 958.8, 968.7, 1043.9, 1244.9, 1369.6, 1473.0, 1654.9, 3146.9, 3152.5, 3231.9, and 3234.3 cm^{-1}. The ab initio harmonic frequencies for C_2H_4, calculated at the highest levels of theory (QCI and MRCI), are in very good agreement with the experimental harmonic frequencies.

Anharmonic vibrational frequencies have been measured[40] and tentatively assigned[41] for C_2H_5. These frequencies are discussed and compared with the ab initio C_2H_5 frequencies in the next section, where the ab initio frequencies for the transition state are also discussed.

C. Reaction Energies. The ab initio reaction energies are summarized in Tables 3 and 4. With the ab initio molecular orbital methods used in the present work, accurate heats of reaction and barrier heights are more difficult to calculate directly than geometries or vibrational frequencies. With the PMP4/6-311+G(2df,p) and QCISD(T)/6-311+G(2df,p) levels of theory the 0 K heat of reaction is 33 kcal/mol, ca. 2−3 kcal/mol less than the best experimental estimates.[5,12,20] Methods that estimate the effects of larger basis sets and correct for higher level electron correlation effects could narrow this gap.[42]

The barrier height for H + C_2H_4 addition is surprisingly difficult to calculate accurately. For the transition state, spin unrestricted Møller−Plesset perturbation theory suffers from serious spin contamination problems, and the barrier is about 10 kcal/mol higher than it should be. Much of this problem

TABLE 3: HF, MP2, and QCISD ab Initio Energies

	6-31G*			6-311G**		6-311+G(2df,p)		
	HF	MP2	QCISD	MP2	QCISD	MP2	PMP4	QCISD(T)
				Total Electronic Energies[a]				
$H + C_2H_4$	−0.529 948	−0.792 516	−0.811 582	−0.881 393	−0.872 720	−0.925 117	−0.923 980	−0.924 864
TS	−0.525 323	−0.772 966	−0.803 026	−0.864 751	−0.866 987	−0.908 650	−0.919 508	−0.919 277
C_2H_5	−0.597 148	−0.844 615	−0.869 044	−0.940 344	−0.938 260	−0.981 105	−0.985 106	−0.985 532
				Reaction Energies[b]				
classical[c]								
$E_{0,f}$	45.07	44.96	41.43	47.44	44.72	45.47	41.16	41.58
$E_{0,r}$	2.90	12.27	5.37	10.44	3.60	10.33	2.81	3.51
ΔH_0	42.17	32.69	36.06	36.99	41.13	35.13	38.36	38.07
quantum[d]								
$E_{0,f}$	39.90	40.89	36.93	43.36	40.14	41.64	36.83	37.24
$E_{0,r}$	3.12	14.04	6.55	12.16	4.59	12.14	3.88	4.58
ΔH_0	36.78	26.85	30.38	31.20	35.55	29.50	32.95	32.66

[a] The total electronic energies are relative to −78.000 000 hartrees. [b] The reaction energies are in kcal/mol. [c] The classical energies do not include zero-point energies. [d] The quantum energies include zero-point energies determined from the harmonic frequencies in Table 2. The QCISD estimated frequencies were used to calculate the PMP4 quantum energies.

TABLE 4: CASSCF and MRCI ab Initio Energies[a]

	total electronic energies[b]		quantum[c]
	$H + C_2H_4$	TS	$E_{0,r}$
CASSCF 3-in-3/DZP	−0.576 241	−0.563 906	8.77
CASSCF 5-in-5/DZP	−0.592 156	−0.582 228	7.26
MRCI/DZP	−0.835 356	−0.827 755	5.80
MRCI/TZP	−0.878 450	−0.872 904	4.61
MRCI/TZP+F	−0.900 237	−0.894 373	4.81
MRCI/TZP//MRCI/cc-pVDZ	−0.878 169	−0.872 339	4.69

[a] The CASSCF and MRCI energies are calculated at the CASSCF and MRCI geometries in Table 1. [b] The total electronic energies are with respect to −78.000 000 hartrees. [c] The difference of the TS and C_2H_4 zero-point energies determined from the harmonic frequencies at the MRCI/cc-pVDZ level of theory (i.e., 1.03 kcal/mol) was used to calculate the quantum $E_{0,r}$. The harmonic frequencies, at the CASSCF/DZP level of theory, give 1.21 kcal/mol for this zero-point energy difference.

can be solved by using an approximate spin projection technique[29] which lowers the barrier by about 7−8 kcal/mol. The QCISD calculations are much less affected by spin comtamination[43] and yield a barrier of 4.6 kcal/mol. The problem of spin contamination can be avoided entirely by using spin restricted multiconfiguration methods. With the basis sets used, the MRCI barrier is similar to the one calculated by QCISD(T). Both approaches give estimates of the barrier that are ca. 2 kcal/mol too high.[5,12,20] Hence, the barrier height and the heat of reaction are taken as adjustable parameters in fitting the experimental rates.

III. Transition State Theory Calculations

A. Molecular and Transition State Geometries and Frequencies. Calculating the transition state theory rate constants for C_2H_5 decomposition and $H + C_2H_4$ recombination requires equilibrium geometries as well as anharmonic vibrational frequencies for C_2H_5, the transition state, and C_2H_4, as well as the 0 K thresholds. Of these properties, only the equilibrium geometry[37] and vibrational frequencies[39] for C_2H_4 are known in total from experiment. The experimental C_2H_4 anharmonic vibrational frequencies are used in the transition state theory calculations, and they are listed in Table 5 along with the C_2H_4 principal moments of inertia calculated from the experimental geometry.[37]

The ab initio calculations are used to determine the equilibrium geometry and anharmonic vibrational frequencies for the transition state. The high-level QCISD/6-311G** and MRCI/cc-pVDZ calculations in the previous section give the most accurate geometries and give a similar geometry for the transition state. For the calculations reported here, the transition state's principal moments of inertia were determined from the QCISD/6-311G** geometry.

The QCISD/6-311G**, MRCI/cc-pVDZ, and estimated QCISD(T)/6-311+G(2df,p) calculations give similar harmonic frequencies for the transition state. Reference harmonic frequencies were assumed to be these QCISD(T) values. Anharmonic frequencies for the transition state were then estimated by multiplying the harmonic frequency for each mode of the transition state by an anharmonic correction factor assumed to be the ratio of the experimental anharmonic frequency and estimated QCISD(T)/6-311+G(2df,p) harmonic frequency for the same type of mode in ethylene. The two modes of the transition state for which there are no analogies in C_2H_4 are the H- - -C═C bends about the rupturing bond. Their scale factor was assumed to be the same as the average of the scale factors for the four CH_2 rocking and bending modes in ethylene. Because of this scaling, the use of the estimated QCISD(T)/6-311+G(2df,p) harmonic frequencies instead of either the QCISD/6-311G** or MRCI/cc-pVDZ harmonic frequencies has no significant effect on the final anharmonic frequencies. The two anharmonic H- - -C═C bend frequencies are 382 and 422 cm^{-1} upon scaling the estimated QCISD(T)/6-311+G(2df,p) harmonic frequencies. These anharmonic frequencies become 367 and 398 cm^{-1} and 395 and 417 cm^{-1} when the QCISD/6-311G** and MRCI/cc-pVDZ harmonic frequencies are scaled, respectively. The anharmonic vibrational frequencies and the principal moments of inertia for the transition state are summarized in Table 5. The vibrational frequencies for the transition state are similar to those proposed previously by HS.[20]

The equilibrium geometry of C_2H_5 is not known from experiment. The most accurate geometry calculated here (see Table 1) is that from the QCISD/6-311G** calculation, which is used to determine the C_2H_5 principal moments of inertia. Ten of the 15 vibrational frequencies of the ethyl radical have been measured[40] and tentatively assigned.[41] Nine of these frequencies and assignments are consistent with the QCISD calculations. The five experimental CH anharmonic stretch frequencies are 3112, 3033, 2987, 2920, and 2842 cm^{-1}. The ratios between these anharmonic frequencies and their analogous QCISD/6-311G** harmonic frequencies vary from 0.9464 to 0.9583 with an average scale factor of 0.9520. Such a factor is expected.[44] The three experimental anharmonic frequencies at 1440, 1366, and 1175 cm−1, assigned here as CH_3 bending (A″), CH_3 bending (A′), and CH_3 rocking (A″), are consistent with their

TABLE 5: Parameters for the Transition State Theory Calculations[a]

	ethyl radical	transition state	ethylene
frequencies, cm^{-1}	3112 (A″)	3113 (A″)	3105 (B_{2u})
	3033 (A′)	3111 (A″)	3103 (B_{1g})
	2987 (A″)	3029 (A′)	3026 (A_g)
	2920 (A′)	3028 (A′)	3021 (B_{3u})
	2842 (A′)	1579 (A′)	1630 (A_g)
	1447 (A′)	1440 (A′)	1444 (B_{3u})
	1440 (A″)	1312 (A′)	1342 (A_g)
	1433 (A′)	1217 (A″)	1220 (B_{1g})
	1366 (A′)	1020 (A″)	1023 (A_u)
	1175 (A″)	988 (A′)	949 (B_{1u})
	1034 (A′)	903 (A′)	940 (B_{2g})
	962 (A′)	820 (A″)	826 (B_{2u})
	783 (A″)	422 (A″)	
	540 (A′)	382 (A′)	
		710i (A′)	
internal rotation moment of inertia, amu·Å^2	1.12[b]		
external rotation moment of inertia, amu·Å^2	24.2, 22.5, 4.92[b]	22.4, 22.2, 6.73[b]	20.4, 16.9, 3.48[c]
symmetry number	6	1	4
0 K quantum barriers, kcal/mol			
$H + C_2H_4 \rightarrow C_2H_5$	3.05		
$C_2H_5 \rightarrow H + C_2H_4$	37.4−40.1		

[a] The frequencies are anharmonic values, and those for the ethyl radical and the transition state were determined by scaling the *ab initio* frequencies; see text. The ethylene anharmonic frequencies are the experimental values.[39] [b] The moments of inertia were calculated from the *ab initio* QCISD/6-311G** geometry. [c] The ethylene experimental geometry, footnote *c* of Table 1, was used to calculate the ethylene moments of inertia.

QCISD harmonic values, i.e., 1508, 1425, and 1214 cm^{-1}. The average experimental anharmonic/QCISD harmonic scale factor for these three modes is 0.9605 and is in accord with previous analyses.[44] The CH_2 umbrella (A′) mode has an experimental anharmonic frequency of 530 cm^{-1}, which is larger than the QCISD harmonic frequency of 455 cm^{-1}. This type of difference is consistent with the expected quartic nature of the umbrella potential.[45]

The ab initio calculations reported here show that the torsional frequency is low, i.e., in the range 120−160 cm^{-1}. A previous ab initio calculation[38] indicated the internal rotational barrier is on the order of 0.5 kcal/mol. These results are consistent with an experimental study[46] suggesting the torsional motion undergoes free internal rotation. Thus, at the high temperatures (T > 700 K) used to study C_2H_5 decomposition, it seems clear the C_2H_5 torsion is a free rotor. This is the model used here.

The experimental C_2H_5 anharmonic frequency of 1138 cm^{-1} and tentatively assigned[41] as the C−C stretch (A′) is inconsistent with the QCISD C−C stretch harmonic frequency of 1077 cm^{-1}. The anharmonic frequency is expected to be lower, and the experimental anharmonic/QCISD harmonic frequency ratio is expected to be in the range ∼0.95−0.96 as given above for the C−H stretch and CH_3 rocking and bending modes. For this work, the QCISD C−C stretch frequency has been scaled by 0.9605 (the CH_3 bending and rocking scale factor) to give a C−C stretch anharmonic frequency of 1034 cm^{-1}. In assigning the experimental C−C stretch frequency, it was pointed out that the assignment is tentative and uncertain.[41]

The four remaining C_2H_5 frequencies, which have not been measured or assigned experimentally, are the CH_2 bending (A′), CH_3 bending (A′), CH_3 rocking (A′), and CH_2 rocking (A″), for which the QCISD/6-311G** harmonic frequencies are 1506, 1494, 1002, and 815 cm^{-1}, respectively. These frequencies were scaled, by the above factor 0.9605, to give the following estimated anharmonic frequencies: 1447, 1433, 962, and 783 cm^{-1}. The principal moments of inertia and anharmonic vibrational frequencies used for the ethyl radical are listed in Table 5. They are similar to those proposed previously by HS.[20]

B. $H + C_2H_4$ Recombination Rate Constant. In this work, the high-pressure $H + C_2H_4$ recombination rate constant is fit by varying the quantum recombination barrier $E_{0,r}$ in a transition state theory calculation. The electronic structure calculations reported here do not give a barrier of quantitative accuracy.[47] The anharmonic vibrational frequencies and principal moments of inertia, given in Table 5 for ethylene and the transition state, are used in the calculation. Both the Eckart[48] and Wigner[49] corrections were used to account for quantum mechanical tunneling. The latter is given by

$$1 + |h\nu/k_B T|^2/24$$

The Eckart tunneling correction depends on three parameters, i.e., the reaction exothermicity, the barrier height, and the second derivative of the vibrationally adiabatic potential at the barrier with the respect to the reaction coordinate. The last parameter is similar to the second derivative of the ab initio potential at the barrier, which gives the imaginary frequency, except zero-point energy for the modes orthogonal to the reaction coordinate are included in the vibrationally adiabatic potential. For the Eckart tunneling correction made here, the experimental 0 K exothermicity of 35.0 kcal/mol is used, while the remaining two parameters were determined from the ab initio calculations.

In analyzing the ab initio barrier heights and curvatures reported here, it was found that a straight line with zero intercept results when the square of the barrier imaginary frequency is plotted versus the classical barrier height for the different ab initio calculations. The barriers (kcal/mol) and imaginary frequencies (cm^{-1}) for this plot are as follows: 3.5, 860.0 [QCISD/6-311+G(2df,p)]; 3.6, 822.5 (QCISD/6-311G**); 4.8, 900.2 (MRCI/DZP); 5.4, 968.1 (QCISD/6-31G*); 6.2, 1176.9 (CASSCF 5-in-5/DZP); and 7.8, 1187.7 (CASSCF 3-in-3/DZP). Since the ab initio values for the barrier height are too large, this plot was used to estimate central barrier curvatures for barrier heights smaller than the ab initio values. The barrier height was then varied in a transition state theory calculation including the Eckart tunneling correction, until the experimental $H + C_2H_4 \rightarrow C_2H_4$ experimental rate constants were fit. The resulting classical barrier height and associated imaginary frequency which fit experiment are 2.00 kcal/mol and 710i cm^{-1}, respectively. The resulting vibrationally adiabatic quantum barrier $E_{0,r}$ is 3.05 kcal/mol. Figure 2 shows there is very good agreement with the rate constants calculated here and the experimental rate constants of Lee et al.,[2] Sugawara et al.,[3] Lightfoot and Pilling,[4] and Hanning-Lee et al.[5] Also plotted in Figure 3 are the rate constants calculated using the estimated QCISD(T)/6-311+G(2df,p) barrier of 4.58 kcal/mol for $E_{0,r}$. The Wigner tunneling correction calculated with the 710i cm^{-1} imaginary frequency and the Eckart tunneling correction are compared in Figure 3.

The quantum barrier of 3.05 kcal/mol deduced here for $H + C_2H_4 \rightarrow C_2H_5$ association is slightly larger than the value of 2.5 kcal/mol deduced by HS. This is because the transition state used here is gives rise to more tunneling than the transition state used by HS. The former has a classical imaginary frequency of 710i cm^{-1}, while for the TS of HS the frequency is 546i cm^{-1}.

C. C_2H_5 Dissociation Rate Constant. As recently discussed by Feng et al.,[12] a consistent set of rate constants has not been

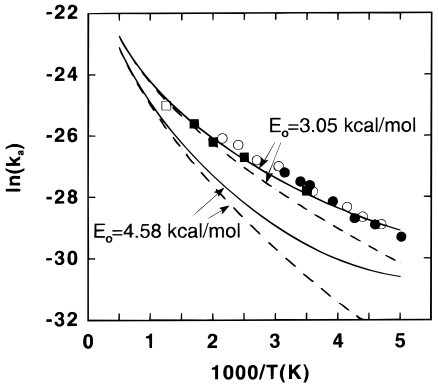

Figure 2. Comparison of calculated and experimental rate constants for $H + C_2H_4$ association at high pressure. Experiment: ●, Lee et al. (1978); ○, Sugawara et al. (1981); ■, Lightfoot and Pilling (1987); □, Hanning−Lee et al. (1992). The solid and dashed lines are the calculated rate constants with and without tunneling, respectively. The rate constants are in units of cm^3 $molecule^{-1}$ s^{-1}.

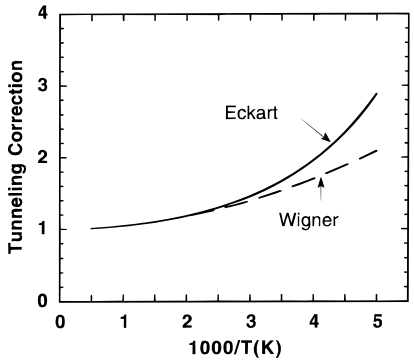

Figure 3. Tunneling corrections used for $H + C_2H_4 \rightarrow C_2H_5$.

measured for the high-pressure unimolecular dissociation of C_2H_5. Instead of attempting to weight the relative accuracy of the different experiments, each of the different sets of experimental rate constants is fit here. This is done by taking the unimolecular barrier $E_{0,f}$ as an adjustable parameter. The anharmonic vibrational frequencies and principal moments of inertia, given in Table 5, for the ethyl radical and transition state are used in the transition state theory calculations. Quantum mechanical tunneling is not important at the high temperatures for C_2H_5 decomposition and was not included in the calculations.

Listed in Table 6 are the rate constants at the lowest, highest, and median temperature of each experimental study. (The median temperature is nearly the same as the temperature found from the median $1/T$, except for the study of Feng et al.[5]) These rate constants were calculated from the experimental Arrhenius parameters, which are listed in Table 3 of ref 5, and from $k(T) = 1.11 \times 10^{10} T^{1.037} \exp(-18504/T)$ s^{-1} recommended by Feng et al. A value for $E_{0,f}$ was chosen to fit the experimental rate constant at the median temperature with TST. This $E_{0,f}$ was then used to determine TST rate constants at the lowest and highest temperatures. Except for the experiments of Trenwith[10] and the $k(T)$ of Feng et al.,[5] there is good agreement between the calculated TST and experimental temperature-dependent rate constants. Feng et al. recommend their $k(T)$ expression for the 200−1100 K temperature range. Here, this $k(T)$ expression is compared with TST calculations for temperatures between 600 and 1000 K. These two limiting temperatures are approximately 100 K lower and higher, respectively, than the temperatures studied in the actual experiments[7−11] of C_2H_5 decomposition.

The experimental and calculated A factors are compared in Table 7. The calculated A factors are larger than those reported by Lin and Back, Simon et al., and Trenwith, but smaller than that reported by Loucks and Laidler. The calculated A factors are approximately 3 times larger than those determined from $k(T)$ expression recommended by Feng et al.[5] The A factors calculated here vary from 1.3 to 1.8 times smaller, for the 400−1000 K temperature range, than the values reported previously by HS.[20] This is because the vibrational frequencies used here for the ethyl radical and transition state are somewhat lower and higher, respectively, than those used by HS.

Overall, the transition state theory calculations give a consistent fit to the data of Lin and Back, Loucks and Laidler, and Pacey and Wimalasena with a value of $E_{0,f}$ which only varies from 37.4 to 38.2 kcal/mol. A larger value for $E_{0,f}$ is required to fit the rates of Simon et al., and a substantially larger value is required to fit the rates of Trenwith. A value for $E_{0,f}$ in the range 37.4−38.2 kcal/mol is consistent with the $E_{0,r}$ value determined here of 3.05 kcal/mol and the "high" value[5] of 28.4 kcal/mol for $\Delta H_{f,298}(C_2H_5)$. This is a weighted average of the "higher" values for the C_2H_5 heat of formation.[5] Taking this value and the 298 K heats of formation for $H^\bullet$ and C_2H_4, which are 52.103 and 12.496 kcal/mol, respectively,[50] gives 36.2 kcal/mol for the 298 K heat of reaction. Correcting for thermal enthalpies yields a 0 K heat of reaction of 35.1 kcal/mol.

TABLE 6: Fits to Experimental C_2H_5 Dissociation Rate Constants

ref	fitted $E_{0,f}$[a] (kcal/mol)	T (K)	k_f^∞ (s^{-1}) expt	k_f^∞ (s^{-1}) TST
Lin and Back[7]	38.2	823	2.2×10^3	2.0×10^3
		868	7.3×10^3	7.3×10^3
		913	2.2×10^4	2.3×10^4
Loucks and Laidler[8]	37.8	673	1.0×10^1	1.1×10^1
		723	8.4×10^1	8.4×10^1
		773	5.3×10^2	5.1×10^2
Simon et al.[9]	38.8	793	5.4×10^2	5.3×10^2
		803	7.3×10^2	7.3×10^2
		813	9.7×10^2	10.0×10^2
Trenwith[10]	40.1	841	1.2×10^3	1.1×10^3
		877	3.0×10^3	3.0×10^3
		913	7.1×10^3	7.9×10^3
Feng et al.[5 b]	38.1	600	3.4×10^{-1}	2.4×10^{-1}
		800	1.0×10^3	1.0×10^3
		1000	1.3×10^5	1.7×10^5
Pacey and Wimalasena[1a]	37.4	902	2.7×10^4	2.7×10^4

[a] $E_{0,f}$ is the quantum mechanical vibrationally adiabatic barrier. [b] The experimental rate constants are calculated from $k(T) = 1.11 \times 10^{10} T^{1.037} \exp(-18504/T)$ s^{-1}, which is recommended for the 200−1100 K temperature range.

TABLE 7: Calculated and Experimental A Factors

T (K)	A factor (s^{-1})	ref
	Calculated	
400	3.4×10^{13}	this work
500	5.0×10^{13}	
600	6.7×10^{13}	
700	8.6×10^{13}	
800	1.1×10^{14}	
1000	1.4×10^{14}	
	Experimental	
823−913	2.7×10^{13}	Lin and Back[7]
673−773	1.9×10^{14}	Loucks and Laidler[8]
793−813	1.6×10^{13}	Simon et al.[9]
841−913	8.9×10^{12}	Trenwith[10]
600	2.5×10^{13}	Feng et al.[5 a]
800	3.4×10^{13}	Feng et al.[5]
1000	4.3×10^{13}	Feng et al.[5]

[a] The A factors are calculated from $k(T) = 1.11 \times 10^{10} T^{1.037} \exp(-18504/T)$, which is recommended for the 200−1100 K temperature range.

Combining this value with $E_{0,r}$ of 3.05 kcal/mol gives 38.15 kcal/mol for $E_{0,f}$.

In comparing the calculated and experimental *A* factors, it should be noted that a dissociation rate is not measured directly in the experiments of Lin and Back[7] and Loucks and Laidler.[8] What is measured is the ratio of the rate constant for ethyl radical dissociation to the square root of the ethyl radical high-pressure recombination rate constant. In their analysis, Feng et al.[12] used the temperature-independent value[51] of 1.8×10^{-11} cm^3 molecule^{-1} s^{-1} for this recombination rate to deduce the experimental *A* factors in Table 7. HS[20] used the slightly higher value of 2.5×10^{-11} cm^3 molecule^{-1} s^{-1}. The use of a temperature-independent rate constant for $2C_2H_5 \rightarrow C_4H_{10}$ is consistent with recent calculations of rate constants for alkyl radical association.[52−55]

IV. Summary

The following conclusions can be drawn from the ab initio and transition state theory calculations reported here.

1. The highest levels of ab initio theory considered here give similar equilibrium geometries and vibrational frequencies. For ethylene, for which the geometry and frequencies have been measured experimentally, the calculated bond lengths differ by less than 0.005 Å and bond angles by less than 0.5° from the experimental values. The ab initio harmonic frequencies for ethylene are 1.01−1.05 times larger than the experimental anharmonic values. A similar relationship is found between the ab initio and experimental frequencies for C_2H_5. This type of agreement between theory and experiment for ethylene and C_2H_5 indicates accurate frequencies and geometries are also calculated for C_2H_5 and the transition state. The single reference CISD and multirefernece CI calculations give a similar geometry and set of vibrational frequencies for both C_2H_5 and the transition state. Because the multireference CI calculation is expected to track differential electron correlation effects accurately,[47] this result also indicates that accurate properties are calculated for C_2H_5 and the transition state.

2. The geometry and types of vibrational modes for the transition state are similar to those for ethylene. Thus, for each mode of the transition state, except the two H- - -C═C bends, there is an equivalent mode in ethylene. Thus, the experimental anharmonic/ab initio harmonic frequency ratio for an ethylene mode was used to estimate the anharmonic frequency for the equivalent mode in the transition state. This scale factor for the H- - -C═C bends was assumed to be the same as that for CH_2 rocking and deformation modes, i.e., 0.98. The H- - -C═C bend frequencies in the transition state are estimated as ∼400 cm^{-1}. The geometry and vibrational frequencies for the transition state are similar to those proposed previously by HS.[20]

3. Ten of the ethyl radical's 15 vibrational frequencies have been measured and assigned.[30] On average the experimental anharmonic C−H stretch frequencies are 0.95 times the ab initio harmonic frequencies. Similarly, the experimental CH_3 rocking and bending frequencies are 0.96 times the ab initio values. This latter scale factor was used to estimate anharmonic frequencies for four of the modes not identified experimentally. The ethyl radical torsion is treated as a free rotation. The ab initio calculations indicate the C−C stretch mode has been misassigned,[40,41] and the previous experimental anharmonic value of 1138 cm^{-1} has been changed to 1034 cm^{-1}. Finally, the experimental anharmonic/ab initio harmonic frequency ratios for C_2H_5 are similar to those for C_2H_4.

4. The ab initio calculations do not give quantitative values for the $H + C_2H_4$ recombination and C_2H_5 dissociation barriers. These barriers were adjusted to fit the experimental rate constants. A consistent set of rate constants have been measured for $H + C_2H_4$ recombination, which can be fit near quantitatively with transition state theory using the transition state properties derived here and a recombination barrier $E_{0,r}$ of 3.0−3.1 kcal/mol. This barrier is nearly the same as that previously deduced by HS.[20]

5. A consistent set of experimental rate constants has not been determined for C_2H_5 dissociation. The transition state derived here, with a dissociation barrier $E_{0,f}$ in the range 37.4−38.2 kcal/mol, gives transition state theory rate constants which fit the data of Lin and Back,[7] Loucks and Laidler,[8] and Pacey and Wimalsena.[11] This $E_{0,f}$ is smaller than those which fit the data of Simon et al.[9] and Trenwith.[10] An $E_{0,f}$ in the range 37.4−38.2 kcal/mol, combined with $E_{0,r}$ of 3.0−3.1 kcal/mol, is consistent with the higher values for the ethyl radical heat of formation.

The analysis reported here emphasizes the need for an accurate calculation of the $C_2H_5 \rightleftharpoons H + C_2H_4$ reaction energetics by ab initio methods and a consistent set of experimental C_2H_5 dissociation rate constants. This information will allow a definitive test of the accuracy of transition state theory for $C_2H_5 \rightleftharpoons H + C_2H_4$.

Acknowledgment. The research reported here was funded by NSF Grants CHE-9400678 and CHE-9403780 and ONR Mechanics Division Grant N000149310045. This paper was written while Bill Hase visited the Reinhard Schinke research group at the Max-Planck-Institut für Strömungsforschung in Göttingen, Germany.

References and Notes

(1) Cowfer, J. A.; Michael, J. V. *J. Chem. Phys.* **1975**, *62*, 3504.
(2) Lee, J. H.; Michael, J. V.; Payne, W. A.; Stief, L. J. *J. Chem. Phys.* **1978**, *68*, 1817.
(3) Sugawara, K.; Okuzaki, K.; Sato, S. *Chem. Phys. Lett.* **1981**, *78*, 259; *Bull. Chem. Soc. Jpn.* **1981**, *54*, 2872.
(4) Lightfoot, P. D.; Pilling, M. J. *J. Phys. Chem.* **1987**, *91*, 3373.
(5) Hanning-Lee, M. A.; Green, N. J. B.; Pilling, M. J.; Robertson, S. H. *J. Phys. Chem.* **1993**, *97*, 860.
(6) Davies, J. W.; Pilling, M. J. In *Bimolecular Reactions*; Ashfold, M. N. R., Baggott, J. E., Eds.; The Royal Society of Chemistry: London, 1989.
(7) Lin, M. C.; Back, M. H. *Can. J. Chem.* **1966**, *44*, 2357.
(8) Loucks, L. F.; Laidler, K. J. *Can. J. Chem.* **1967**, *45*, 2795.
(9) Simon, Y.; Foucaut, J. F.; Scacchi, G. *Can. J. Chem.* **1988**, *66*, 2142.
(10) Trenwith, A. B. *J. Chem. Soc., Faraday Trans. 2* **1986**, *82*, 457.
(11) Pacey, P. D.; Wimalasena, J. H. *J. Phys. Chem.* **1984**, *88*, 5657.
(12) Feng, Y.; Niiranen, J. T.; Benosura, A.; Knyazev, V. D.; Gutman, D.; Tsang, W. *J. Phys. Chem.* **1993**, *97*, 871.
(13) Sloane, C. S.; Hase, W. L. *Faraday Discuss. Chem. Soc.* **1977**, *62*, 210.
(14) Hase, W. L.; Mrowka, G.; Brudzynski, R. J.; Sloane, C. S. *Faraday Discuss. Chem. Soc.* **1978**, *69*, 3548; **1980**, *72*, 6321.
(15) Hase, W. L.; Wolf, R. J.; Sloane, C. S. *J. Chem. Phys.* **1979**, *91*, 211; **1982**, *76*, 2771.
(16) Hase, W. L.; Buckowski, D. G. *J. Comput. Chem.* **1982**, *3*, 335.
(17) Hase, W. L.; Buckowski, D. G.; Swamy, K. N. *J. Phys. Chem.* **1983**, *87*, 2754.
(18) Hase, W. L.; Ludlow, D. M.; Wolf, R. J.; Schlick, T. *J. Phys. Chem.* **1981**, *85*, 958.
(19) Swamy, K. N.; Hase, W. L. *J. Phys. Chem.* **1983**, *87*, 4715.
(20) Hase, W. L.; Schlegel, H. B. *J. Phys. Chem.* **1982**, *86*, 3901.
(21) Schlegel, H. B. *J. Phys. Chem.* **1982**, *86*, 4878.
(22) Schlegel, H. B.; Bhalla, K. C.; Hase, W. L. *J. Phys. Chem.* **1982**, *86*, 4883.
(23) See for example the discussions in refs 1, 6, 12, and 20.
(24) Castelhano, A. T.; Marriott, P. R.; Griller, D. *J. Am. Chem. Soc.* **1981**, *103*, 4262.
(25) Zhu, L.; Hase, W. L. *Chem. Phys. Lett.* **1990**, *175*, 117.
(26) Zhu, L.; Chen, W.; Hase, W. L.; Kaiser, E. W. *J. Phys. Chem.* **1993**, *97*, 311.
(27) Hariharan, P. C.; Pople, J. A. *Theor. Chim. Acta* **1973**, *28*, 213 and references cited. Francl, M. M.; Pietro, W. J.; Hehre, W. J.; Binkley, J. S.; Gordon, M. S.; DeFrees, D. J.; Pople, J. A. *J. Chem. Phys.* **1982**, *77*,

3654. Frisch, M. J.; Pople, J. A.; Binkley, J. S. *J. Chem. Phys.* **1984**, *80*, 3265 and references cited.
(28) Møller, C.; Plesset, M. S. *Phys. Rev.* **1934**, *46*, 618.
(29) Schlegel, H. B. *J. Chem. Phys.* **1986**, *84*, 4530; *J. Phys. Chem.* **1988**, *92*, 3075.
(30) Pople, J. A.; Head-Gordon, M.; Raghavachari, K. *J. Chem. Phys.* **1987**, *87*, 5968.
(31) Frisch, M. J.; Trucks, G. W.; Head-Gordon, M.; Gill, P. M. W.; Wong, M. W.; Foresman, J. B.; Johnson, B. G.; Schlegel, H. B.; Robb, M. A.; Replogle, E. S.; Gomperts, R.; Andres, J. L.; Raghavachari, K.; Binkley, J. S.; Gonzalez, C.; Martin, R. L.; Fox, D. J.; Defrees, D. J.; Baker, J.; Stewart, J. J. P.; Pople, J. A. *GAUSSIAN 92*; Gaussian, Inc.: Pittsburgh, PA, 1992.
(32) Roos, B. O.; Taylor, P. R.; Siegbahn, P. E. M. *Chem. Phys.* **1980**, *48*, 152.
(33) Dunning, T. H., Jr. *J. Chem. Phys.* **1970**, *53*, 2823. Dunning, T. H.; Hay, P. J. In *Modern Theoretical Chemistry*; Schaefer, H. F., III, Ed.; Plenum Press: New York, 1977; Vol. 3.
(34) Huzinaga, S. *J. Chem. Phys.* **1965**, *42*, 1293.
(35) Dunning, T. H., Jr. *J. Chem. Phys.* **1989**, *90*, 1007.
(36) Saxe, P.; Lengsfield, B. H.; Martin, R.; Page, M. MESA (Molecular Electronic Structure Applications), The University of California, 1990.
(37) Duncan, J. L. *Mol. Phys.* **1974**, *28*, 1177.
(38) Pacansky, J.; Dupuis, M. *J. Chem. Phys.* **1978**, *68*, 4276.
(39) Duncan, J. L.; McKean, D. C.; Mallinson, P. D. *J. Mol. Spectrosc.* **1973**, *45*, 221.
(40) Pacansky, J.; Dupuis, M. *J. Am. Chem. Soc.* **1982**, *101*, 415.
(41) Pacansky, J.; Schrader, B. *J. Chem. Phys.* **1983**, *78*, 1033.
(42) Curtiss, L. A.; Jones, C.; Trucks, G. W.; Raghavachari, K.; Pople, J. A. *J. Chem. Phys.* **1990**, *93*, 2537. Curtiss, L. A.; Raghavachari, K.; Trucks, G. W.; Pople, J. A. *J. Chem. Phys.* **1991**, *94*, 7221. Curtiss, L. A.; Carpenter, J. E.; Raghavachari, K.; Pople, J. A. *J. Chem. Phys.* **1992**, *96*, 9030.
(43) Chen, W.; Schlegel, H. B. *J. Chem. Phys.* **1994**, *101*, 5957.
(44) Thomas, R. J.; Deleeuw, B. J.; Vacek, G.; Schaefer, III, H. F. *J. Chem. Phys.* **1993**, *98*, 1336. Pople, J. A.; Scott, A. P.; Wong, M. W.; Radom, L. *Isr. J. Chem.* **1993**, *33*, 345. East, A. L. L.; Allen, W. D.; Klippenstein, S. J. *J. Chem. Phys.* **1995**, *102*, 8506.
(45) Duchovic, R. J.; Hase, W. L.; Schlegel, H. B. *J. Phys. Chem.* **1984**, *88*, 1339.
(46) Pacansky, J.; Coufal, J. *J. Chem. Phys.* **1980**, *72*, 5285.
(47) Bauschlicher, Jr., C. W.; Langhoff, S. R.; Taylor, P. R. *Adv. Chem. Phys.* **1990**, *77*, 103.
(48) Eckart, C. *Phys. Rev.* **1930**, *35*, 1303.
(49) Steinfeld, J. I.; Francisco, J. S.; Hase, W. L. *Chemical Kinetics and Dynamics*; Prentice-Hall: Englewood Cliffs, NJ, 1989; p 318.
(50) Stull, D. R.; Prophet, H. *Natl. Stand. Ref. Data Serv.* **1971**, *Natl. Bur. Stand. No. 37*.
(51) Tsang, W.; Hampson, R. F. *J. Phys. Chem. Ref. Data* **1986**, *15*, 1087.
(52) Hu, X.; Hase, W. L. *J. Chem. Phys.* **1991**, *95*, 8073.
(53) Barbarat, P.; Accary, C.; Hase, W. L. *J. Phys. Chem.* **1993**, *97*, 11706.
(54) de Sainte Claire, P.; Barbarat, P.; Hase, W. L. *J. Chem. Phys.* **1994**, *101*, 2476.
(55) Song, K.; de Sainte Claire, P.; Hase, W. L.; Hass, K. C. *Phys. Rev. B* **1995**, *52*, 2949.

JP9528875